Unified description of collective nuclei with the interacting boson model

W.-T. Chou,[1,2,3] N. V. Zamfir,[2,3,4,5] and R. F. Casten[2]
[1]*National Tsing Hua University, Hsinchu, Taiwan, Republic of China*
[2]*Wright Nuclear Structure Laboratory, Yale University, New Haven, Connecticut 06520*
[3]*Brookhaven National Laboratory, Upton, New York 11973*
[4]*Clark University, Worcester, Massachusetts 01610*
[5]*Institute of Atomic Physics, Bucharest Magurele, Romania*
(Received 14 March 1997)

It was recently demonstrated that the empirical linear correlation of $E(4_1^+)$ with $E(2_1^+)$ is reproduced by the interacting boson model 1 (IBA-1) if a constant value for the coefficient κ of the $\mathbf{Q}\cdot\mathbf{Q}$ term is used. This constancy motivates the present investigation of whether it is possible to find sets of IBA-1 parameters, with fixed κ, that reproduce the data for a more general set of observables and a wide range of nuclei. A consistent procedure, based on contour plots of key observables, was used to extract ϵ and χ values for 145 nuclei spanning the $Z = 50$–82 shell, which give reasonable overall agreement with the data with smoothly varying parameters. The constant κ constraint sometimes leads to parameter values different than normal: finite ϵ values ($\sim$ 0.1 MeV) even for rotational nuclei and large χ values for transitional and vibrational nuclei that even increase towards the vibrational region. Finally, a systematic correlation of ϵ values with $E(2_1^+)$ was found. [S0556-2813(97)04808-5]

PACS number(s): 21.10.Re, 21.60.Fw, 27.60.+j, 27.70.+q

I. INTRODUCTION

Countless interacting boson approximation (IBA) calculations have been done over the last 20 years, and the model [1] has proved to be a valuable interpretive and predictive aid in understanding nuclear structure and its evolution as a function of N, Z, and A. The model has entered the lexicon of standard approaches to nuclear structure.

Recently, it was found that all collective (but nonrotational) medium mass and heavy nuclei display a remarkably compact linear correlation of yrast energies with $E(2_1^+)$ [2]. In particular, $E(4_1^+)$ values are linear with $E(2_1^+)$ with an empirically fit slope of 2.00 ± 0.02. IBA-1 calculations reproduce this linearity with an extremely broad range of parameters provided that the coefficient κ of the $\mathbf{Q}\cdot\mathbf{Q}$ term in the Hamiltonian is kept constant [3]. (The magnitude of this constant determines the intercept of the linear correlation: For nuclei in the entire region $Z = 38$–82, the empirical value of the intercept is 0.16 ± 0.01 MeV, which requires $\kappa = 0.032 \pm 0.002$ MeV.)

There is, of course, no *a priori* requirement that κ be constant. The same linear correlation could also be reproduced, nucleus by nucleus, by simultaneously adjusting κ, ϵ, and χ, in the IBA Hamiltonian. However, this is far more complicated than the simple *Ansatz* of constant κ, in which case the linearity becomes virtually automatic and nearly parameter independent.

Historically, IBA calculations for collective nuclei have adjusted the parameters to fit each nucleus with no special constraints. As a consequence, a variety of κ values have been invoked. The reproduction of the empirical yrast energy correlation mentioned above by the IBA, and the recent analytic interpretation of this result in terms of a simple phonon excitation scheme [4], suggests that it would be worthwhile to revisit IBA calculations for collective nuclei within the framework of a constant κ *Ansatz* to determine if it is possible to reproduce the properties (including nonyrast excitations) of these nuclei with such a constraint: that is, to determine if satisfactory ϵ and χ values exist for constant κ that give fits to the data, comparable to those obtained previously, and, if so, to determine whether these ϵ and χ values vary in a smooth and reasonable way with N and Z across a broad region of the nuclear chart. To further expand the scope of this investigation and to test the generality of a constant κ perspective, we have also included rotational nuclei in this study of all collective nuclei with $Z = 50$–82.

There is a secondary point to this study. Traditionally, IBA calculations have usually been carried out either for individual nuclei or for sequences of related nuclei (e.g., isotopic chains). Different studies used different prescriptions and approaches to the choices of parameters, ranging from simplifying *Ansätze* based on external arguments, either phenomenological or microscopic, to multiparameter least squares fits. It would clearly be of interest to apply a consistent set of criteria to a broad range (in mass and structure) of nuclei so that the parameters are determined within a consistent framework.

The usefulness and philosophy of such an approach are fourfold. First, such parameters would provide gross predictions of the structure of virtually any nucleus. Such predictions have many uses in themselves, ranging from understanding the evolution of structure to providing input for astrophysical network calculations. Second, such predictions give useful guides to poorly studied nuclei that can be helpful in designing future experiments. An obvious case in point, of current interest, is in new nuclei that will become accessible with radioactive nuclear beams (RNB's). It is likely that the first RNB experiments in a new region will obtain only the most rudimentary data. Whether or not more thorough experiments are warranted, and how best to design

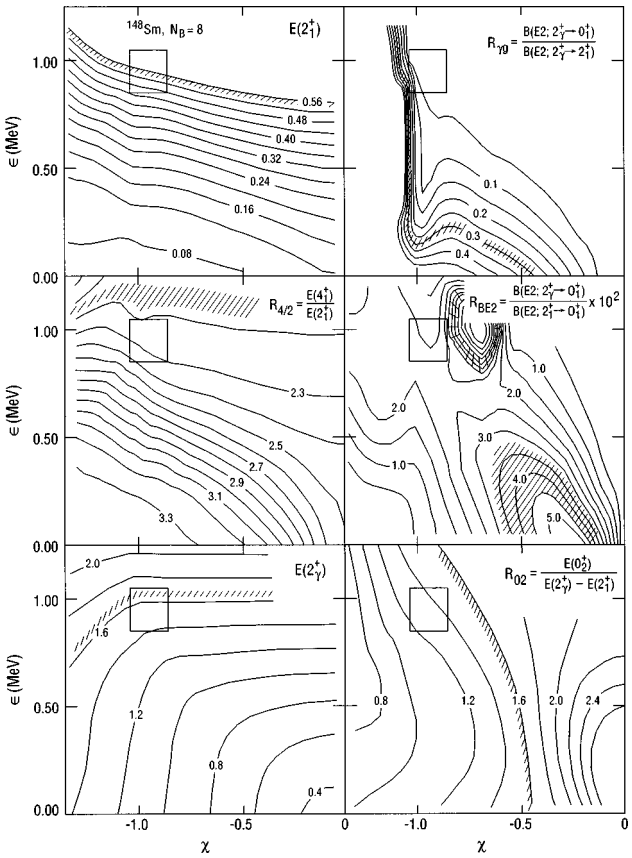

FIG. 1. Contour plots of different observables in the (χ,ϵ) plane for $N_B=8$. The theoretical values are indicated on the curves (the energies are in MeV). The experimental values of each observable in ^{148}Sm are shown as crosshatched bands of values (see text for details). The square areas denote the best choice of χ and ϵ considering all the observables.

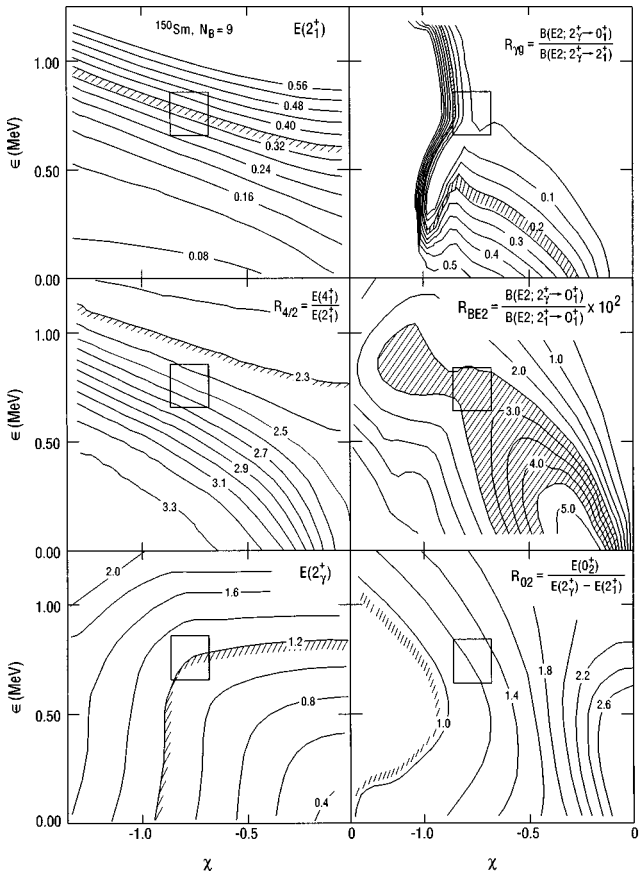

FIG. 2. The same as Fig. 1 but for $N=9$ and ^{150}Sm.

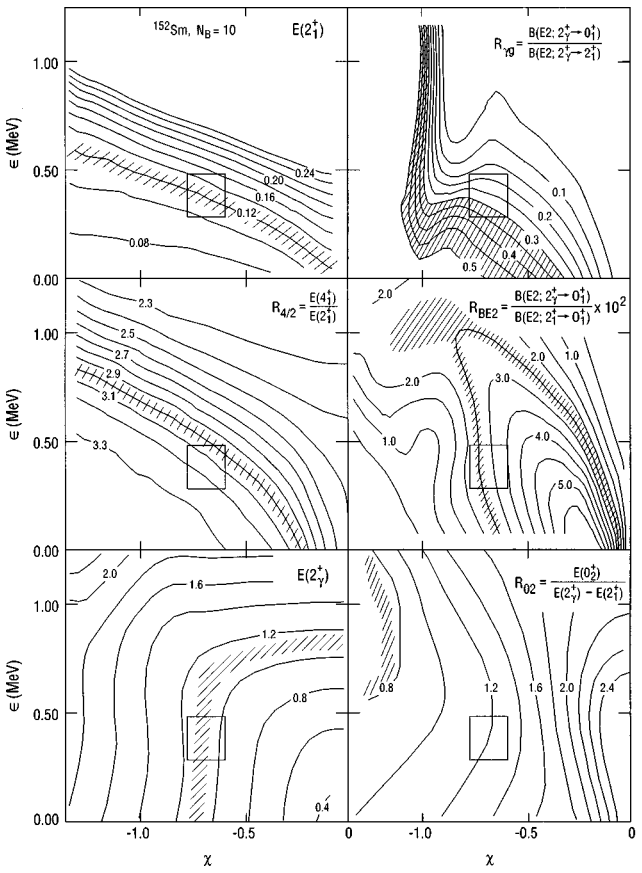

FIG. 3. The same as Fig. 1 but for $N=10$ and ^{152}Sm.

them, can be aided by standardized IBA calculations. Third, such parameter sets can also serve as good starting points for more detailed fits to individual nuclei to test the IBA more stringently. Fourth, owing to the use of a constant κ *Ansatz*, the parameter sets and the variations in parameter values that we obtain can be easily compared with microscopic derivations of the model parameters and, thereby, can help to better understand the underlying rationale for the model.

It is therefore our purpose in this paper to apply a set of standard criteria for IBA-1 calculations, expressed in the form of contour plots of predictions for various key collective observables, as a function of two parameters ϵ and χ to a large body of nuclei from $A\sim 120$ to 200—specifically, all collective even-even nuclei ($R_{4/2}\geqslant 2.0$) with $Z=54$–78 and $N\geqslant 66$, with boson number $N_B=4$–16. In all, 145 nuclei are included in this survey. The data are from the Nuclear Data Sheets with a cutoff date at the end of 1996. For each nucleus two to six such contour plots are used (depending on the amount and quality of the data available). A similar method has recently been used, but with different goals and criteria, by Harder and Tang [5].

II. METHOD AND RESULTS

It is well known that a few key observables give a reasonable overall perspective on the (low-spin) structure of a

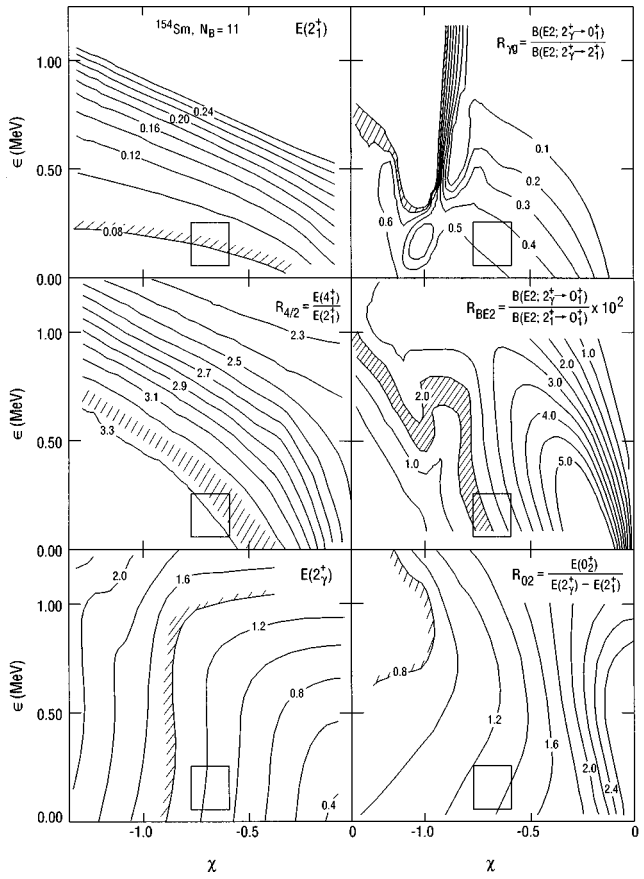

FIG. 4. The same as Fig. 1 but for $N=11$ and ^{154}Sm.

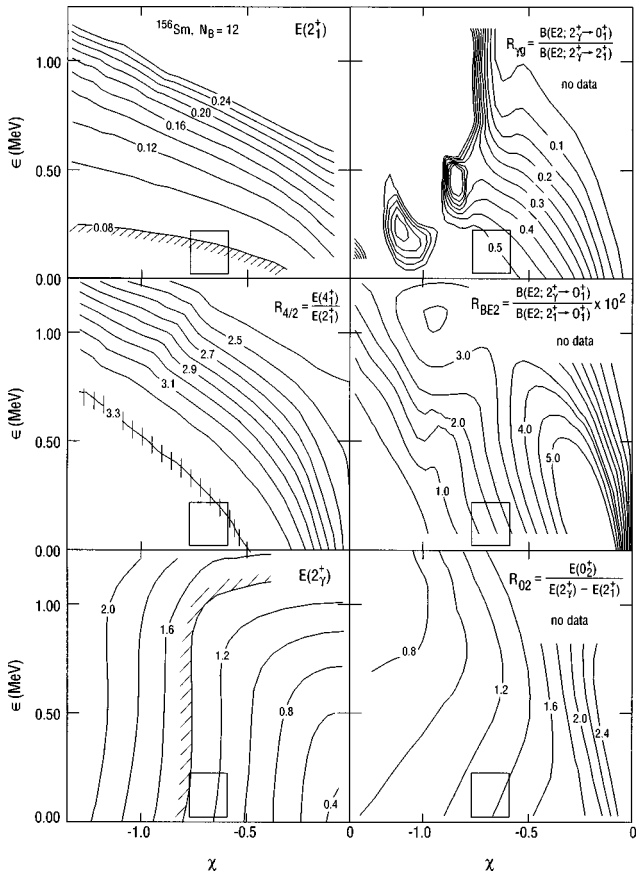

FIG. 5. The same as Fig. 1 but for $N=12$ and ^{156}Sm.

typical collective even-even nucleus. The most useful are (in an obvious notation) $E(2_1^+)$, $R_{4/2}=E(4_1^+)/E(2_1^+)$, $E(2_\gamma^+)$ where the 2_γ^+ state is usually the bandhead of the quasi γ band, or else a member of the two-phonon-like multiplet, $R_{02}=E(0_2^+)/[E(2_\gamma^+)-E(2_1^+)]$, $R_{\gamma g}=B(E2;2_\gamma^+\rightarrow 0_1^+)/B(E2;2_\gamma^+\rightarrow 2_1^+)$, and $R_{BE2}=B(E2;2_\gamma^+\rightarrow 0_1^+)/B(E2;2_1^+\rightarrow 0_1^+)$. Fortunately, these observables are also among the easiest to measure.

We use the IBA-1 in the extended consistent **Q** formalism (ECQF) in which the Hamiltonian takes the form [6]

$$H=\epsilon n_d-\kappa Q\cdot Q, \tag{1}$$

where

$$Q=(s^\dagger\tilde{d}+d^\dagger s)+\chi(d^\dagger\tilde{d})^{(2)} \tag{2}$$

and the electric quadrupole operator $T(E2)=e_B Q$.

The parameters are ϵ, χ, and κ. (Since we consider only ratios for the $E2$ transition rates the effective boson charge e_B cancels out.) In the three dynamical symmetries these three parameters take on the values U(5): $\kappa=0$, $\chi=0$; O(6): $\epsilon=0$, $\chi=0$; SU(3): $\epsilon=0$, $\chi=-\sqrt{7}/2$. In typical deformed nuclei, one often uses the simpler consistent **Q** formalism (CQF) with $\epsilon=0$. We will see, however, that, with fixed κ, it is necessary to use finite ϵ values even for rotor nuclei, just as vibrational nuclei will be seen to have improved fits if both ϵ and χ are finite and even sometimes reasonably large.

Equations (1) and (2) involve three parameters plus the boson number N_B, defined as half the number of valence

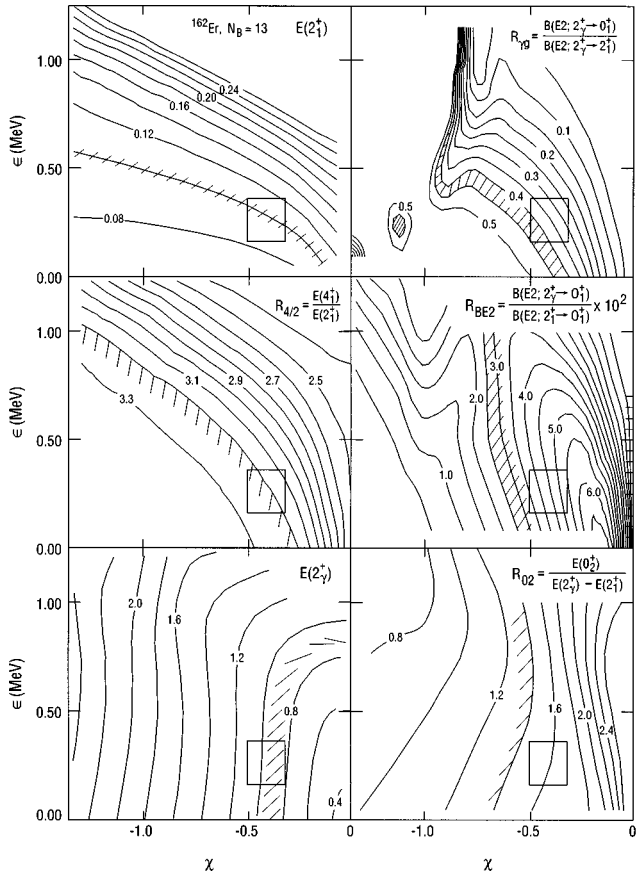

FIG. 6. The same as Fig. 1 but for $N=13$ and ^{162}Er.

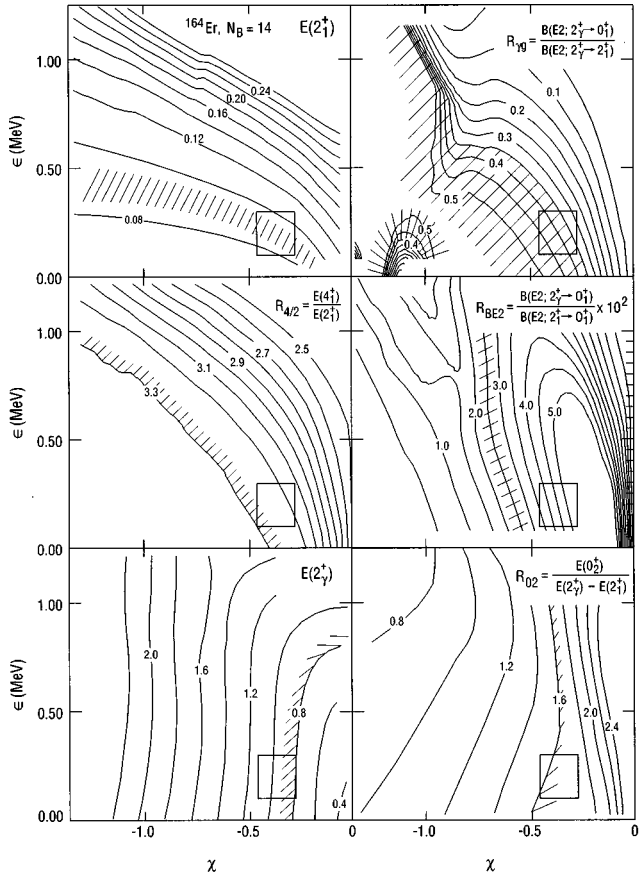

FIG. 7. The same as Fig. 1 but for $N=14$ and ^{164}Er.

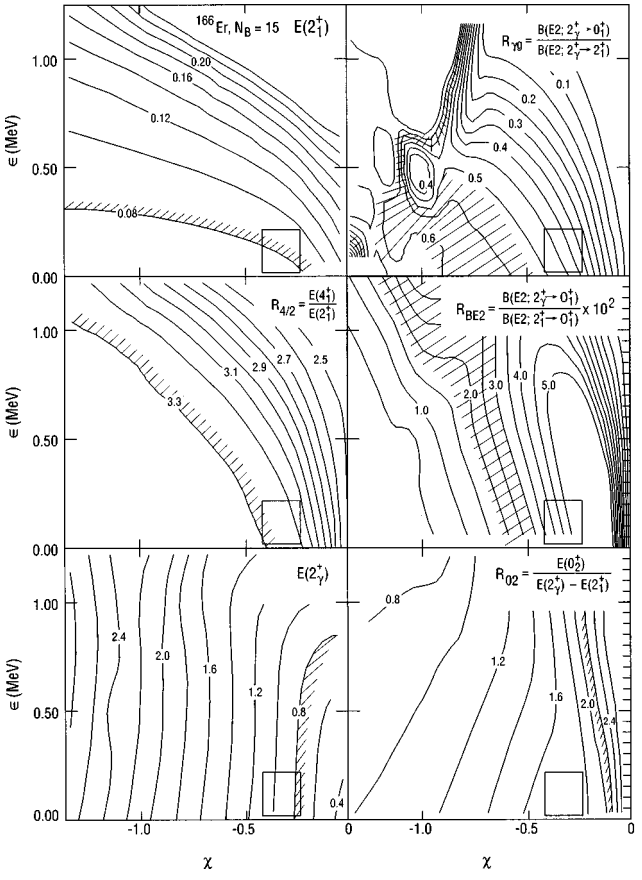

FIG. 8. The same as Fig. 1 but for $N=15$ and ^{166}Er.

protons and neutrons, each taken separately relative to the nearest closed shell. We obtain the boson numbers N_B, using the standard magic numbers 50, 82, and 126. (A discussion of the use of the $Z=64$ closure will also be made below.) We fix κ at 0.03 MeV. The procedure leaves ϵ and χ as free parameters and we deduce them from the contour plots. For each N_B (N_B = 4–16) we carried out approximately 80 calculations for a mesh of ϵ and χ values and constructed the results for each observable in the form of a contour plot. Examples of these contour plots are shown in Figs. 1–9 and, in each, the empirical values of each observable are shown as crosshatched bands of values. The nuclei in Figs. 1–9 are chosen to show the variety of levels of agreement, ranging from quite good to cases where no set of parameters reproduces all the observables and where a compromise fit is therefore indicated.

We will now inspect a couple of these in more detail to show the procedures used.

Consider Fig. 2 for ^{150}Sm. This is a transitional nucleus with $E(2_1^+)=0.334$ MeV. This experimental value is shown as the sloping band of hatching in the upper left panel of Fig. 2. The finite width of the band (larger than the experimental error) reflects the fact that, in assessing any model, one must make realistic demands on the model. For example, if we expect a model to predict both energies and branching ratios (BR's) (for allowed transitions, say) with comparable accuracy, we would consider acceptable calculated energies within a few percent of the absolute values. In this situation the typical experimental energy uncertainties of a fraction of a keV are not the relevant criterion. Similarly, for BR's in-

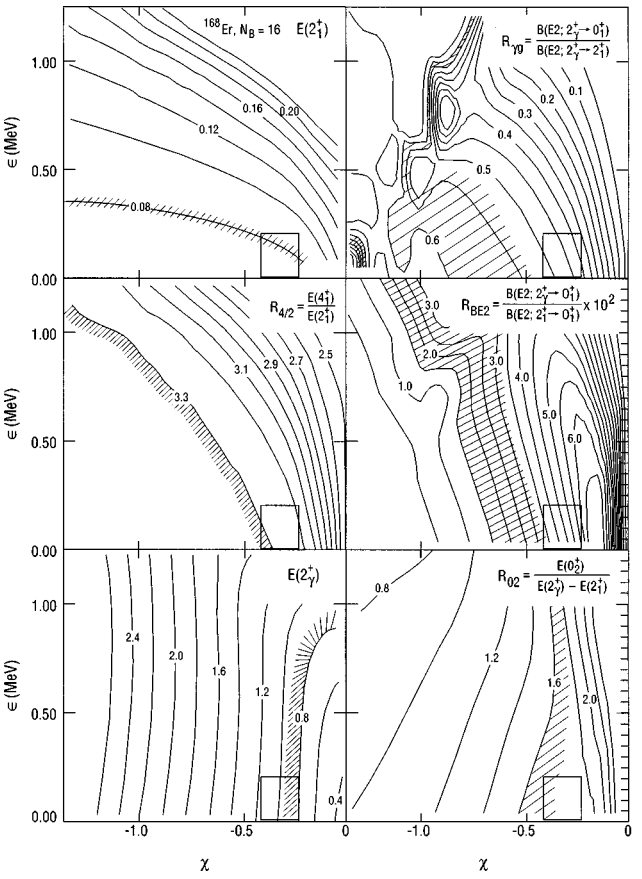

FIG. 9. The same as Fig. 1 but for $N=16$ and ^{168}Er.

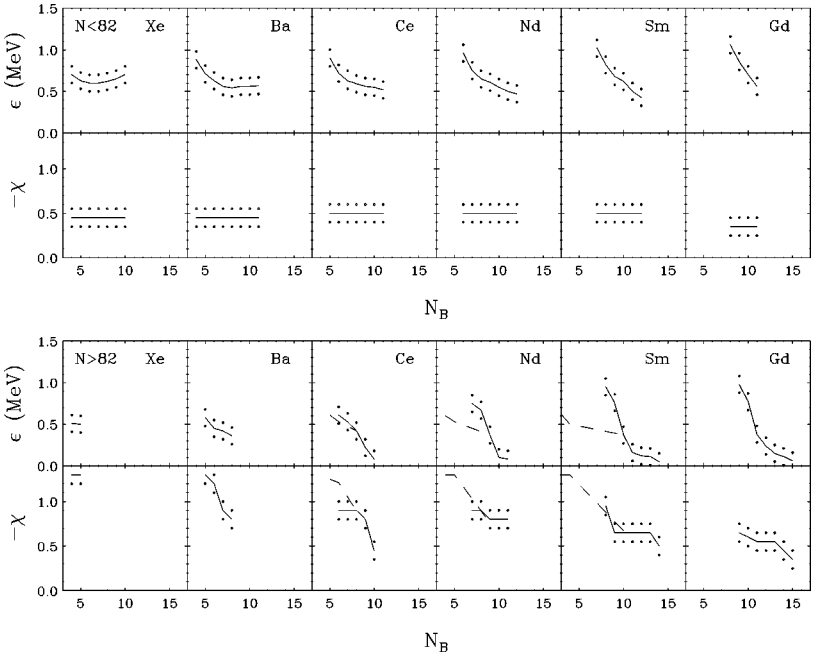

FIG. 10. The parameters ϵ and χ (solid lines) obtained from contour plots for isotopes in the $52<Z<66$ region as a function of boson number N_B. The dotted lines show the range of values consistent with the contour plots for all observables included in the analysis. The dashed lines in the bottom panels ($N>82$) are the parameters obtained considering a $Z=64$ subshell closure for $N<90$.

volving weak or forbidden transitions that are sensitive to small components in the wave function, we would normally be pleased with agreement of calculations within, say, a factor of 2. For example, for a measured BR of 0.5, a calculated value of 1.0 misses much of the physics, but if the observed BR is 0.02, a calculation giving 0.04 nicely reproduces the relative forbiddeness of the numerator. The widths of the empirical bands of values in Figs. 1–9 reflect these criteria.

Returning to Fig. 2, the observed $E(2_1^+)$ value is consistent with nearly any χ as long as ϵ is in the range 0.6–1.0 MeV. The $R_{4/2}$ ratio gives nearly the same result, albeit tending toward a preference for ϵ values in the upper part of this range. The $E(2_\gamma^+)$ data effectively rule out any χ values more negative than -1.0 while being consistent with the other data on the best choice for ϵ. The BR $R_{\gamma g}$ reiterates this limit on χ. The R_{02} ratio makes it clear that χ must be more negative than about -0.8. The R_{BE2} ratio is also consistent with all the above considerations, all of which give a best fit range of parameter values $\epsilon\sim$ 0.65–0.85 MeV and $\chi\sim-0.7\rightarrow-0.8$. We stress in this discussion that the ϵ and χ values, regardless of how consistent the data are, should not be considered defined or determined to better than a range of values of roughly $\pm$ 0.1 MeV and $\pm$ 0.1, respectively. The square areas denoting the best choices of ϵ and χ in Figs. 1–9 are of this size. For ^{150}Sm, the overall agreement is quite good: Each hatched square touches or nearly touches the data value.

Consider as another example the deformed nucleus ^{164}Er (Fig. 7). Here, the lower $E(2_1^+)$ value requires ϵ values lower (regardless of χ) than $\sim$ 0.5 MeV while $E(2_\gamma^+)$ requires that χ be no more negative than -0.5 and, in fact, for all ϵ from 0–0.6 MeV, that χ is ~-0.35. In conjunction with $E(2_1^+)$ this then determines that $\epsilon\sim$0.2 MeV. The other data are consistent.

In some cases, it is impossible to find a consistent set of ϵ and χ values. In general, the worst agreement is for the always enigmatic 0_2^+ states (the observable R_{02}), for which no models work well. In other cases (e.g., $R_{\gamma g}$,R_{BE2}, and

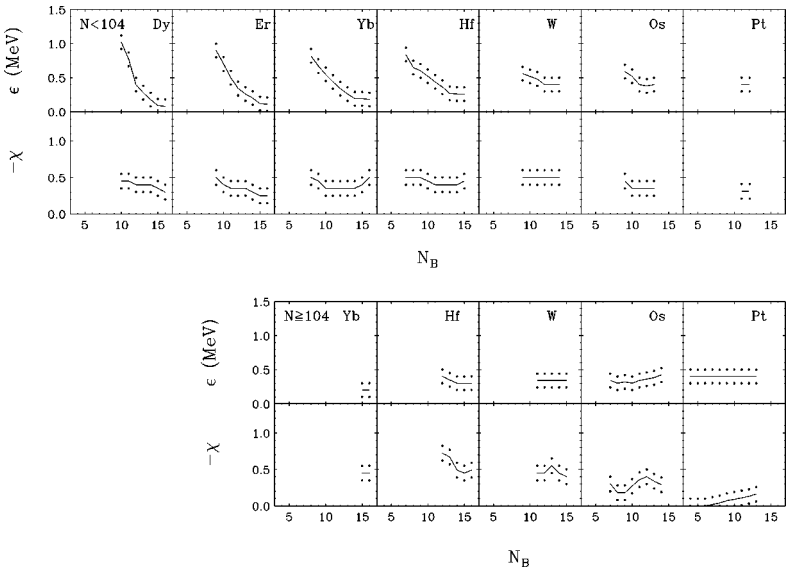

FIG. 11. The same as Fig. 10 but for $66\leqslant Z<80$ (upper panels $N<104$ and lower panels $N\geqslant 104$).

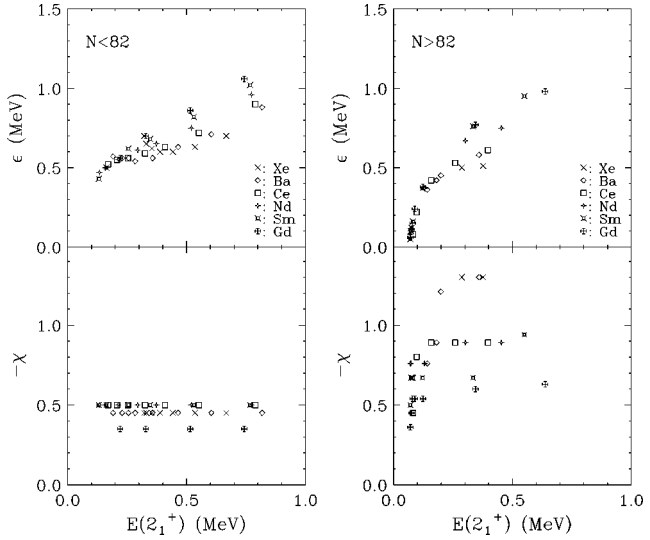

FIG. 12. The parameters ϵ and χ obtained from contour plots for isotopes in the $52<Z<66$ region as a function of the experimental $E(2_1^+)$ values (the panels on the left-hand side for $N<82$ and those on the right-hand side for $N>82$).

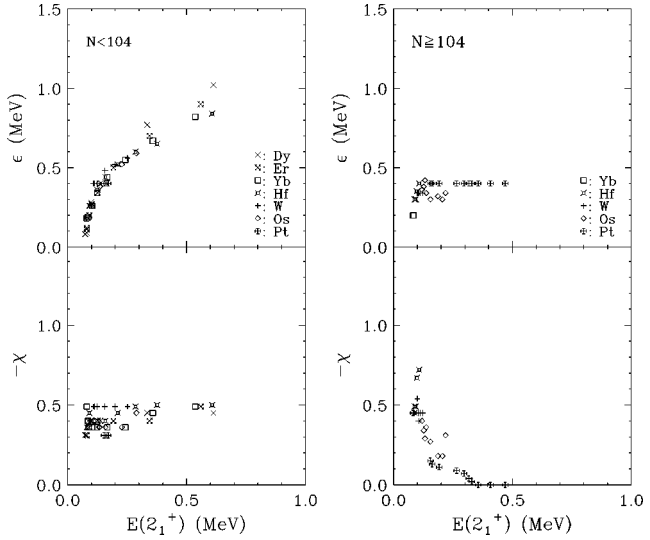

FIG. 13. The same as Fig. 12 but for $66\leqslant Z<80$ (left-hand side for $N<104$ and right-hand side for $N\geqslant 104$).

R_{02} for ^{156}Sm) no data are available. In a few nuclei (e.g., Ce, Nd with $N_B = 11$, W with $N<104$) only $E(2_1^+)$ and $R_{4/2}$ are known. In themselves, these do not sufficiently constrain ϵ and χ. In these cases, we were guided by the properties of similar neighboring nuclei.

We summarize the parameters obtained for each nucleus in Figs. 10 and 11. In Figs. 12 and 13 the parameters are plotted in a compact and revealing way against $E(2_1^+)$. Some comments are perhaps useful. First of all, we note the overall smoothness of the parameters. Some of the trends are as expected. For example, typically ϵ decreases as boson numbers increase and the nuclei become more rotational. For low $E(2_1^+)$, ϵ increases rapidly with increasing $E(2_1^+)$ and, then, for $E(2_1^+) \gtrsim 0.15$ MeV, ϵ becomes nearly linear in $E(2_1^+)$ with a slope quite close to unity such that, for most nuclei (some neutron-deficient Xe-Ce nuclei and neutron-rich W-Pt nuclei are the exceptions), ϵ (MeV) $\sim 0.300 + E(2_1^+)$ (MeV). In deformed and many transitional nuclei χ values are typically ~ -0.4 (see Figs. 12 and 13). In the Os-Pt region with $N\geqslant 104$ (see Fig. 13) $|\chi|$ strongly decreases with increasing $E(2_1^+)$ as the Pt O(6) region is approached. The $A\sim 150$ region (see Fig. 12) shows more scatter, and involves some subtle issues: Hence we discuss it below at some length.

Some parameter values and trends, in Figs. 12 and 13, are rather unexpected. Perhaps the most interesting are the large $|\chi|$ values in vibrational and transitional nuclei near $A = 150$. In the first half of the rare earth region (Ba-Sm), for $N> 82$, $|\chi|$ values approach or (in Ba) even exceed 0.8. (For the same isotopes, but with $N<82$, χ is nearly rigid at -0.4.) We have carefully verified that such large $|\chi|$ values are indeed optimal [recall, $\chi = 0$ is expected for near U(5) nuclei]. This is illustrated in Fig. 14 for ^{148}Sm. The large $|\chi|$ solution is shown in the second panel from the left. In the third panel, we show the optimum fit obtained with small $|\chi|$, even allowing κ to vary. Clearly, the $B(E2)$ ratio $R_{\gamma g}$ is much better with large $|\chi|$. Also, with small $|\chi|$, the ratio $R_{BE2}(0.0003)$ is much less than the data (0.05). Finally, the experimental ratio $R_{3\gamma g}\equiv B(E2;3_\gamma^+\rightarrow 2_\gamma^+)/B(E2;3_\gamma^+\rightarrow 2_g^+)$ $\leqslant 20$ is consistent with the large $|\chi|$ calculation ($R_{3\gamma g} = 3.3$) but not with the small $|\chi|$ fit ($R_{3\gamma g}\sim 3000$).

These results raise an interesting possibility. Figure 12

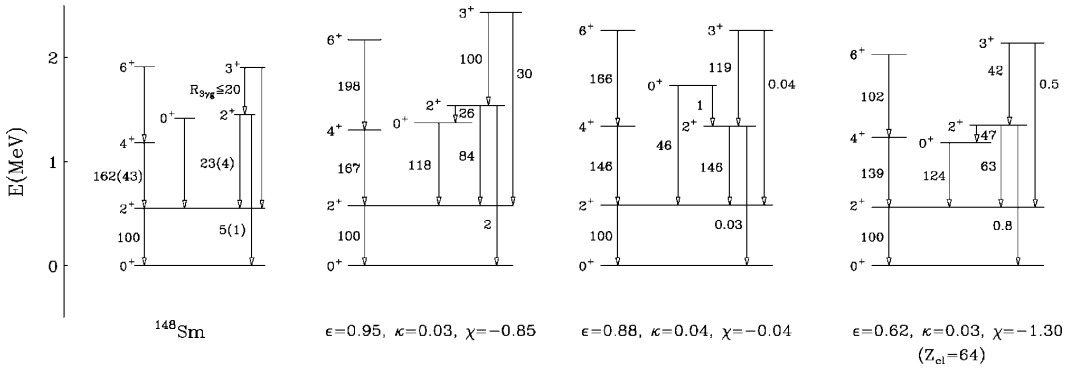

FIG. 14. Experimental low-lying states in ^{148}Sm compared with three sets of IBA calculations: In the leftmost calculation the parameters were obtained from contour plots with fixed κ, the middle calculation is the optimum fit with small $|\chi|$, allowing κ to vary, and the rightmost panel uses $Z=64$ as a shell closure. The experimental ratio $R_{3\gamma g}$ is the branching ratio $B(E2;3_\gamma^+\rightarrow 2_\gamma^+)/B(E2;3_\gamma^+\rightarrow 2_g^+)$. The mixing ratio for the transition in the numerator is unknown: The equals sign in the limit shown in the figure corresponds to a pure $E2$ transition.

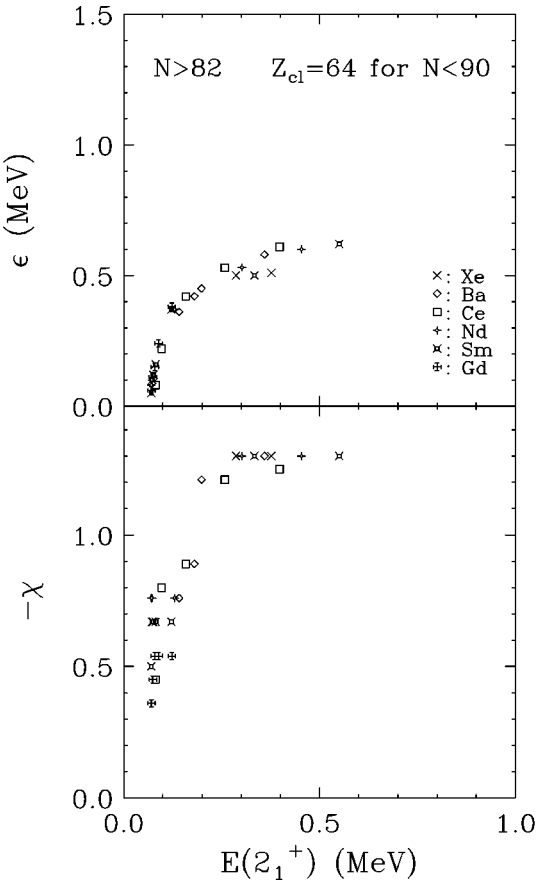

FIG. 15. The same as Fig. 12 left-hand panels but using a $Z=64$ subshell closure in counting boson numbers for $N<90$.

shows that not only are the $|\chi|$ values large for this region (and only for this region) but they also scatter significantly. It may be that this is due to the neglect of the $Z=64$ subshell closure. To test this, we have reconsidered these nuclei assuming a $Z=64$ closure for $N<90$ [7]. In the right panel of Fig. 14 we show the results of the calculation for ^{148}Sm considering $Z_{\rm cl}=64$. The fit also results in large $|\chi|$ and is comparable to that in the second panel and superior to the small $|\chi|$ fit.

Moreover, assuming $Z=64$ is a good subshell closure for $N<90$ gives a much smoother systematics in χ and even a slightly more compact ϵ phenomenology. This is shown in Fig. 15 which should be compared with the more erratic values in Fig. 12. The χ values assuming a subshell closure at $Z=64$ are also given in Fig. 10 as a dashed line: They do not disturb the smooth systematics across the isotopic chains. Interestingly, though, the results obtained assuming a subshell closure at $Z=64$ do *not* change the other feature noted above, namely, the very large magnitude for χ found in these nuclei. (Similar results have also been found for ^{152}Sm by Wilhelm and Radermacher [8].) A microscopic study of these unexpected results is clearly called for.

Another unexpected result is that the optimal ϵ values in deformed nuclei are nonzero: Values of 0.1–0.2 MeV are typical and definitely improve the fits. Kuyucak and Li [9] have also found that the predictions of the IBA in the $1/N$ expansion method for high spin states are improved if a finite ϵ is used, and Barfield and Barrett [10] have used finite ϵ values in calculations of rotational bands in U isotopes. The

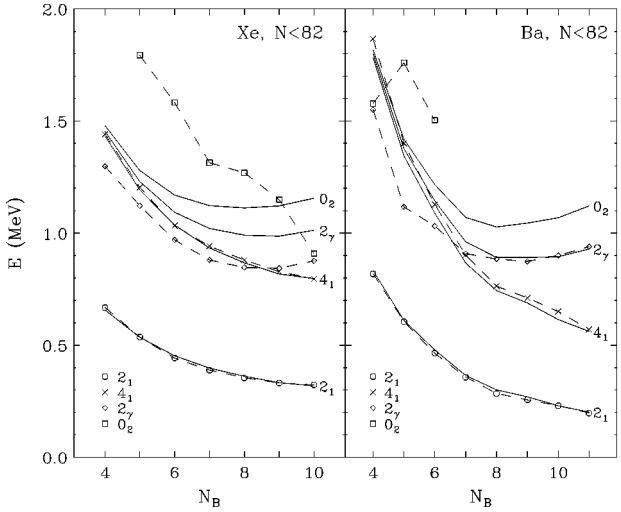

FIG. 16. Comparison between the experimental level energies (symbols connected by dashed lines) and the IBA calculations (connected by solid lines) for Xe and Ba isotopes with $N<82$.

large $|\chi|$ and ϵ values in the neutron-deficient Xe-Ba region are also interesting. These nuclei have historically been considered good O(6) nuclei [11] which would suggest $\epsilon, \chi = 0$. This particular result, and its relation to the constant κ constraint, will be discussed at more length in a forthcoming paper [12].

Of course, it is important to remember that these results are not inconsistent with other IBA calculations that used small $|\chi|$ values in vibrational nuclei and negligible ϵ values in deformed nuclei. Our results are a direct consequence of the constraint of constant κ and are a measure of the implications of such an *Ansatz*.

It is useful to see how the level of agreement for each pair of ϵ and χ values from Figs. 10 and 11 translates into traditional level schemes. To look at the results in this way, we consider Figs. 16–20. The agreement is generally good with the general exception of the 0_2^+ level. For this level, the calculation generally follows the *trend* in energies but the absolute values are often quite far off.

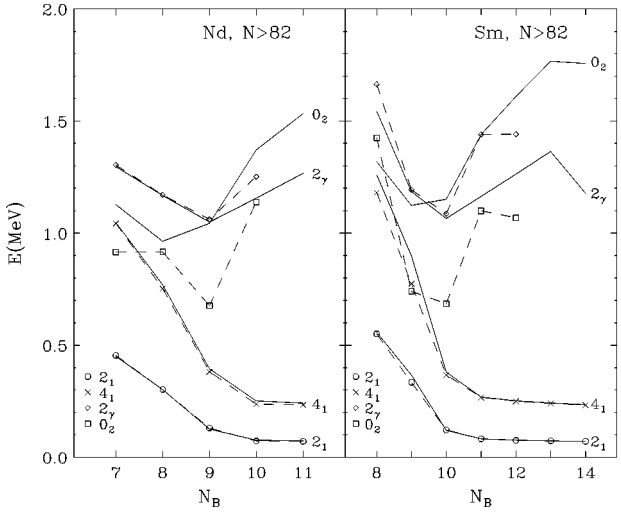

FIG. 17. The same as Fig. 16 but for Nd and Sm isotopes with $N>82$.

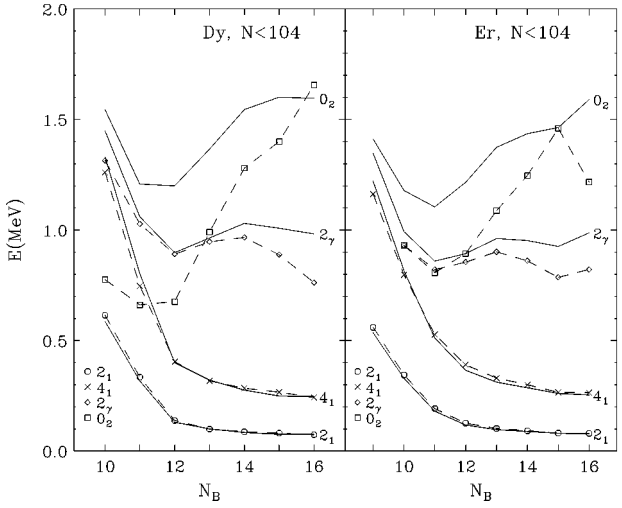

FIG. 18. The same as Fig. 16 but for Dy and Er isotopes with $N<104$.

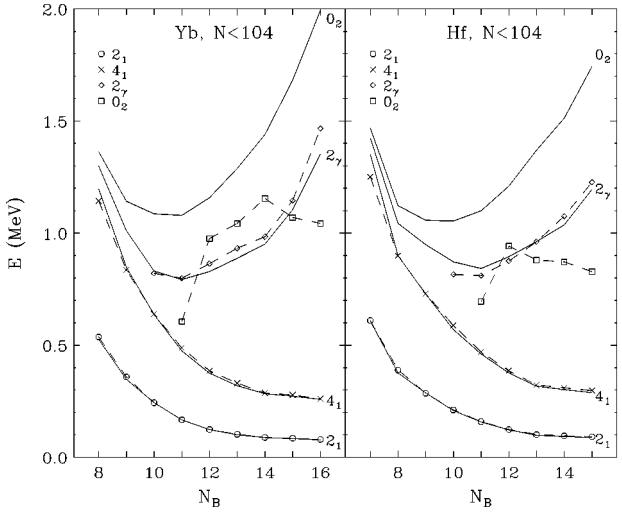

FIG. 19. The same as Fig. 16 but for Yb and Hf isotopes with $N<104$.

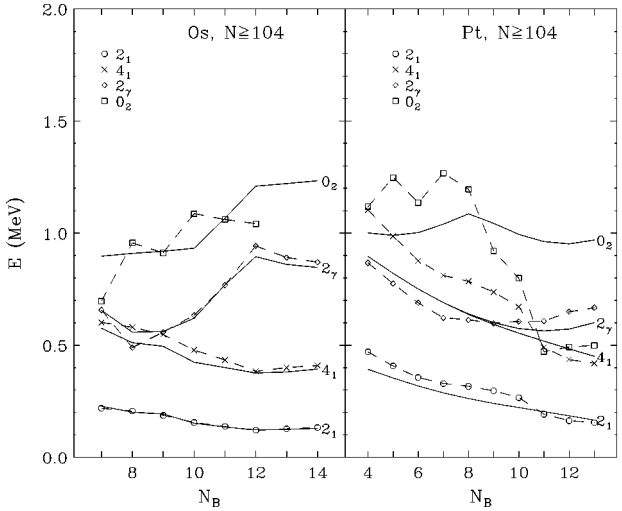

FIG. 20. The same as Fig. 23 but for Os and Pt isotopes with $N\geqslant 104$.

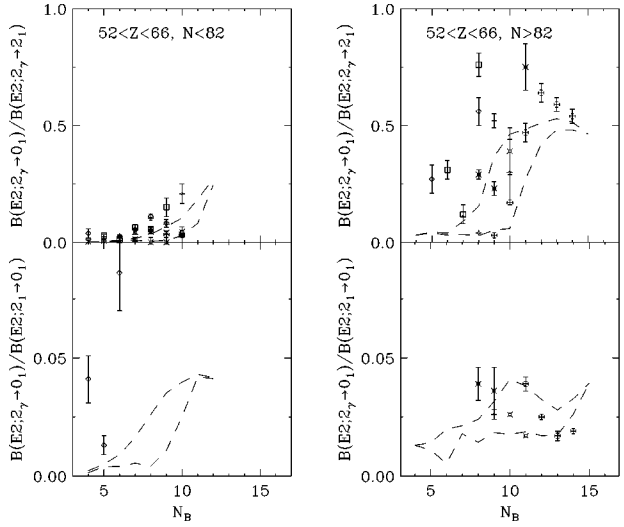

FIG. 21. Experimental $B(E2)$ ratios for isotopes with $52<52<66$ (the panels on the left-hand side for $N<82$ and on the right-hand side for $N>82$) compared with the IBA calculations. The dashed lines represent the extreme values obtained with the parameters from contour plots irrespective of Z. Here and in Fig. 22, the symbols have the same meanings as in the corresponding Figs. 12 and 13.

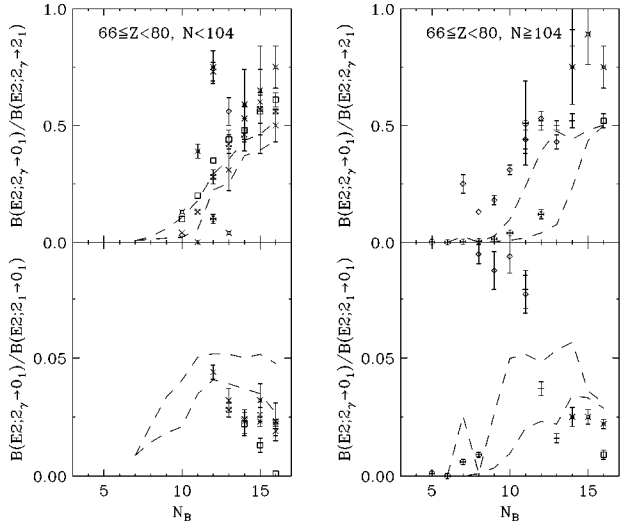

FIG. 22. The same as Fig. 21 but for $66\leqslant Z<80$ (left-hand side for $N<104$ and right-hand side for $N\geqslant 104$).

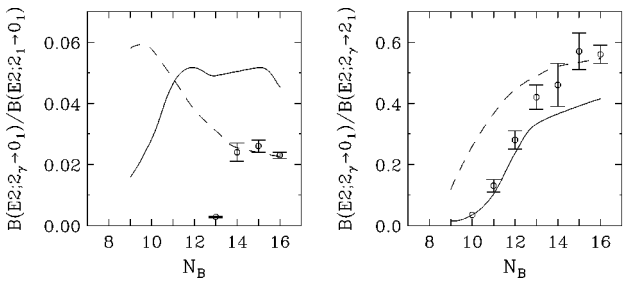

FIG. 23. Comparison of the experimental $B(E2)$ ratios in Er isotopes (symbols) with two IBA calculations: present ECQF calculations (solid lines) and CQF calculations (i.e., $\epsilon=0$) (dashed lines).

The 0_2^+ states remain an enigma in virtually all models and their structure is still largely unknown. Traditionally called β vibrations, in fact a number of them decay predominantly to the γ vibration and there has been discussion of whether or not they might have significant double-γ character [13]. Clearly, more research is needed on these states and the difficulties experienced by the IBA calculations are typical of the current understanding of them.

It is also interesting to determine if the systematic variation of parameters accounts for the $B(E2)$ ratios. The $B(E2)$ ratios in Figs. 21 and 22 do generally show the same trends as the data. For the BR on the left, which vanishes in U(5) and O(6), and approaches the Alaga ratio of 0.7 in the large N_B limit for a rotor Hamiltonian, the experimental trend is more or less reproduced although the calculations on average underestimate the ratios somewhat. The $B(E2)$ ratio on the right is always small (< 0.1) since the denominator is a very collective phonon or intraband rotational transition while the numerator is either forbidden, highly hindered, or an interband transition. Therefore, one hopes for and expects only approximate agreement from a model, that is, small values for this branching ratio. In this regard, the calculations are reasonable, giving ratios that are never more than about 0.06 which is the same range as for the data although detailed agreement is elusive.

The motivation for the calculations in this paper is the fact that the IBA reproduces the linear $E(4_1^+)$ vs $E(2_1^+)$ relation found empirically if κ is kept constant and the extension of this *Ansatz* to rotational nuclei. As the parameter values obtained show finite ϵ values for well deformed nuclei, the question naturally arises as to the relation between the present calculations and standard ones for such nuclei. We illustrate the comparison of the present ECQF (CQF with ϵ term) calculations with CQF calculations [14] for the Er nuclei in Fig. 23, for two important $B(E2)$ ratios. (Both calculations show comparable levels of agreement with the energies.) Although the two sets of calculations behave differently in the left-hand panel, the agreement is comparable. Moreover, overlaps of the wave functions in the two calculations are high ($\sim$ 0.80–0.95) for deformed nuclei, except for the excited 0^+ states. Clearly, to distinguish a preference for one approach or the other on the basis of these $B(E2)$ values would require new data in the light, neutron-deficient Er isotopes where the effects of the ϵ term are greatest.

III. CONCLUSIONS

We have carried out calculations for 145 nuclei in the $Z=50$–82 shell from $A=120$ to 200 with the IBA-1 using a consistent set of procedures and a standarized set of six observables. Using the extended CQF and a constraint of constant κ, which is motivated by the linear correlation of $E(4_1^+)$ with $E(2_1^+)$, we extracted optimal ϵ and χ values for each nucleus by combining the results of contour plots for each of these observables. Generally, pairs of ϵ and χ values reasonably consistent with each of the observables could be obtained. In some cases, no consistent solution resulted and some compromise was necessary in the choice of ϵ and χ. Overall, the agreement of calculated energy and $E2$ transition rate observables with the data is reasonable. The main exceptions are the 0_2^+ states whose structure is still poorly understood.

The parameter values obtained are interesting in themselves. In deformed nuclei we found a need for small but finite ϵ values (typically 0.1–0.2 MeV). Even slightly higher ϵ values are needed for optimal fits to O(6)-like nuclei. Perhaps the most surprising result is the large $|\chi|$ values ($\gtrsim 0.8$) found for vibrational and transitional nuclei in the mass $A\sim 150$ region and the frequently *increasing* trend in $|\chi|$ as boson number *decreases*, as opposed to common perception. This presumably reflects the effects of imposing the constraint of constant κ. Finally, another interesting result is a nearly linear behavior of ϵ with $E(2_1^+)$ for most transitional and vibrational nuclei studied. Indeed, a good approximation to the results for ϵ is the simple expression ϵ (MeV) $= 0.300 + E(2_1^+)$ (MeV) for $E(2_1^+) \gtrsim 0.15$ MeV.

These results can be useful in testing microscopic calculations of IBA parameters. They can serve as starting points for more detailed fits to specific nuclei. By extrapolation of the parameter trends, they can provide estimates for the properties of inaccessible nuclei for use, for example, in astrophysical calculations or as guidance in the design of experiments on new nuclei with radioactive beams. Finally, along with the striking empirical linearity of $E(4_1^+)$ with $E(2_1^+)$, which is most naturally reproduced in the IBA by assuming constant κ, they provide a means of assessing both the rationale or justification of a constant κ *Ansatz* and of assessing its usefulness in IBA calculations.

ACKNOWLEDGMENTS

We are grateful to P. von Brentano, P. Petkov, A. Dewald, and I. Wiedenhöfer for useful and interesting discussions. This work was supported under Contract Nos. DE-AC02-76CH00016, DE-FG02-91ER0609, and DE-FG02-88ER40417 with the U.S. Department of Energy.

[1] A. Arima and F. Iachello, Phys. Rev. Lett. **35**, 1069 (1975).
[2] R. F. Casten, N. V. Zamfir, and D. S. Brenner, Phys. Rev. Lett. **71**, 227 (1993).
[3] N. V. Zamfir and R. F. Casten, Phys. Lett. B **341**, 1 (1994).
[4] R. V. Jolos, P. von Brentano, R. F. Casten, and N. V. Zamfir, Phys. Rev. C **51**, R2298 (1995).
[5] M. K. Harder and K. T. Tang, Phys. Lett. B **369**, 1 (1996).
[6] P. O. Lipas, P. Toivonen, and D. D. Warner, Phys. Lett. **155B**, 295 (1985).
[7] R. F. Casten, D. D. Warner, D. S. Brenner, and R. L. Gill, Phys. Rev. Lett. **67**, 1433 (1981).
[8] M. Wilhelm and E. Radermacher (private communication).

[9] S. Kuyucak and S. C. Li, Phys. Lett. B **354**, 189 (1995).
[10] A. F. Barfield and B. R. Barrett, Nucl. Phys. **A557**, 551 (1993).
[11] R. F. Casten and P. von Brentano, Phys. Lett. **152B**, 22 (1985).
[12] N.V. Zamfir, W.-T. Chou, and R.F. Casten (unpublished).
[13] R. F. Casten and P. von Brentano, Phys. Rev. C **50**, R1280 (1994).
[14] D. D. Warner and R. F. Casten, Phys. Rev. Lett. **48**, 1385 (1982).